Iraqi Journal of Agricultural Sciences –2026:57(5):1389-1401
P-ISSN: 0075- 0530 /E-ISSN: 2410-0862
DOI: https://doi.org/10.36103/se82k705

SPATIAL VARIABILITY OF HEAVY SAND MINERALS IN AL-KARMA REGION, AL-ANBAR GOVERNORATE, IRAQ

Shireen Mudhafar Ali Alkhalil*, Bilal Majeed Kareem Almashhadani
Abdulghafour Ibrahim Hamad Sawsan Ahmed Mohammed,
Department of Desertification Combat, College of Agricultural Engineering Sciences, University of Baghdad, Baghdad, Iraq

ABSTRACT

This study aims to analyze the mineral composition in the AL-Karmah area in the Anbar Governorate in western Iraq, within the flood plain of the Euphrates River, bounded between 33°23'00" and 33°25'00" north, and 43°53'00" and 43°56'00" East, with an area of 54451.14 hectares. 25 surface samples with a depth of 0-30 cm were collected. Bromoform was used to separate heavy minerals from light minerals. The mineral composition was using diagnosis polarized microscope. The ArcMap GIS software analyzed the spatial distribution and produced maps using IDW method. The results of the geographical analysis of the distribution of heavy minerals in the soils of the Karma area showed the dominance **of specific ratios of several minerals. Iron oxides (45.76–48.17%) covered the largest area, amounting to 59.04%. While chlorite percentage was (7-10%) in 87.72% of the whole area. Garnet (5-8%) dominated 86.91%, and zircon (3-6%) dominated 96.34%. Pyroxene (5-8%) covered 63.08%, and amphibole (3-5%) scored 93.08%. As for the epidote (4-6%), it amounted to 97.64%. Muscovite (3-6%) was found in 92.39%, while biotite (4-6%) dominated 96.82% of the area.**

Keywords: inverse distance method IDW, mineral composition, polarized microscope.

Received: 22/3/2025, Accepted: 25/6/2025, Published: 30/5/2026

INTRODUCTION

The optimal use of agricultural land is one of the essential components for achieving high productivity in agroecosystems. To achieve this goal, a comprehensive soil survey is of great importance, in which they are classified into diverse systems .This process provides accurate information about the physical and chemical soil properties are spatial variability such as: particle size, bulk density, Electric conductivity, organic matter, Minerals. Moreover, detailed maps can be prepared highlighting the characteristics of the soil, including its degree of development and productive potential, which mainly contributes to determining the most effective methods of soil exploitation (Jubair *et al.*, 2019.). That the study of the mineral composition of sand and silt particles is very important for understanding the origin and genesis of soils, because these particles are caused by the natural crushing of rocks of origin without chemical transformation (Mange and Maurer, 1992). Thus, this process facilitates the study of the origin and development of soils, as well as transport and sedimentation processes. Also, studying the distribution of sand and silt minerals in different soil layers and determining their depth reflects the homogeneity of the material of origin (AlKhalil and Essa.2020; Issa, 2022). Minerals resistant to weathering do not change much during soil formation processes, therefore, the system of their distribution in the soil is largely constant. Based on this constant distribution, this could indicate that the soil was formed from a single parent material (Chen *et al.*, 2024). Heavy minerals such as Zircon, Tourmaline, Garnet, and Rutile, and light minerals such as Quartz and Feldspar, are

Iraqi Journal of Agricultural Sciences –2026:57(5):1389-1401
P-ISSN: 0075- 0530 /E-ISSN: 2410-0862
DOI: https://doi.org/10.36103/se82k705

among the most prominent indicators in determining the homogeneity of the earth. The predominant minerals in Iraqi soils include opaque minerals such as ultramafic, Epidote, Amphiboles, and Pyroxenes, with a few percentages of Garnet and Zircon minerals. The Al-Karma region in Al-Anbar Province provides a favorable sedimentary environment for studying the distribution of heavy sand minerals. Located within the Euphrates River floodplain, the area is rich in mineral deposits shaped by sedimentary processes and water flow. The high density of heavy minerals causes them to accumulate in low-energy zones like floodplains, where river currents significantly influence their spatial distribution which contribute to the transport and deposition of heavy minerals. Al-Karma is located about 16 km east of the city of Fallujah, and its geographical coordinates are precisely determined between the of 33°23'00" and 33°25'00" north, and 43°53'00" and 43°56'00" East. 25 surface samples were collected from the topsoil at a depth of 0-30 cm. The locations of these samples were determined using a global positioning device (GPS). The study area was represented, and sample locations were mapped using the geographic information systems (ArcMap GIS v10.8) software to create an accurate spatial distribution that contributes to the reliable analysis of geological and mineralogical results.

(Saber *et al* 2021). Therefore, this study aims to analyze the mineral composition of heavy sand minerals in Al-Karma region, determine and draw the spatial distribution of heavy sand minerals in the soil of the study area using the method of spatial interpolation IDW.

MATERIALS and METHODS

Office work (1): The area of Al-Karma Figure1, located at the Al- Anbar province western of Iraq, was chosen as the location for the study, as it is part of the floodplain of the Euphrates River. Its richness in mineral deposits is due to the influence of local sedimentary characteristics as well as water and river currents

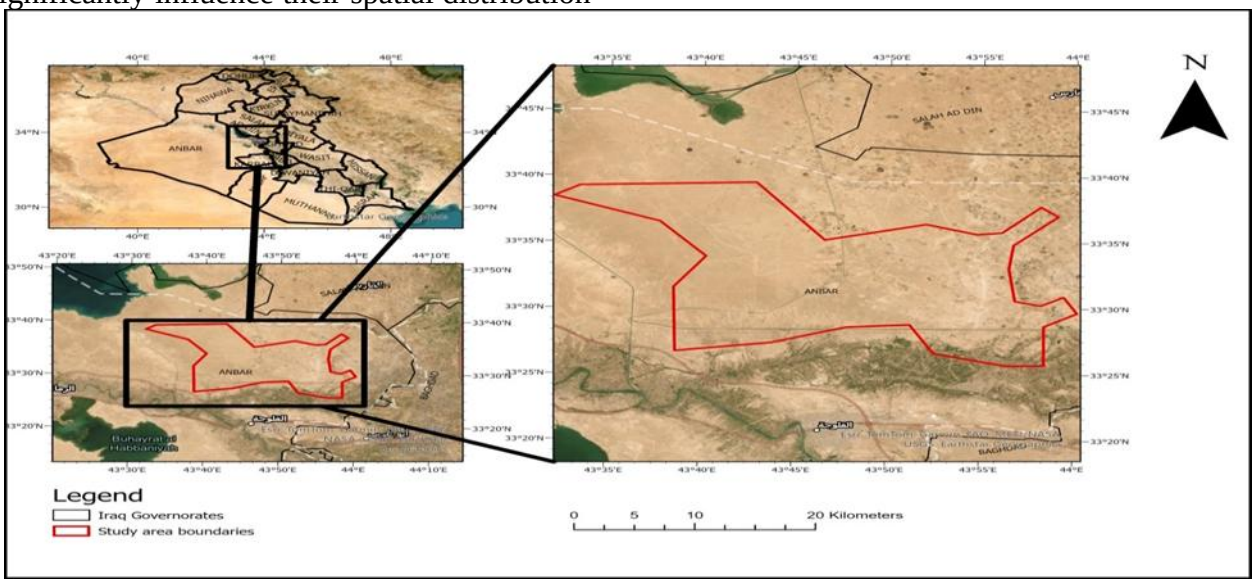

Figure 1. The study area.

Laboratory work: Sand particles were separated into light and heavy minerals using the approved bromoform method (Brewer, 1976). The composition of heavy minerals was determined using the standard counting technique via a polarizing microscope. The samples were separated and air-dried, and then weighed for the same purpose. A separation funnel with bromoform (CHBr3), having a specific gravity of 2.89, was used to separate heavy minerals from light minerals in samples. The sand fractures were studied by polarized light microscopy according to the (Hesse, 1971), while the complete mineral composition of the samples was determined in the laboratory of the Department of Geology-College of Sciences University of Baghdad.

Iraqi Journal of Agricultural Sciences –2026:57(5):1389-1401
P-ISSN: 0075- 0530 /E-ISSN: 2410-0862
DOI: https://doi.org/10.36103/se82k705

Office work (2): A table of the ratios heavy sand minerals was created as a data base to map the Spatial variability of it depending IDW method, with determination of the areas occupied by these ratios in the study area.

RESULTS and DISCUSSION

1- Mineral composition of heavy minerals of sand: Table (1) reveals a diverse assemblage of heavy minerals, dominated by opaque minerals, followed by garnet, amphiboles, pyroxene, and mica. Mixed mineral assemblages were also detected, though some lacked diagnostic optical properties. Opaque minerals outperformed the rest of the minerals in all studied soil horizons, ranging from 42.1-57%. This distribution is due to the observed the influence of both the source material and the transport mechanism (Khedr *et al*., 2023). The presence of a group of flaky minerals, such as Chlorite, in proportions ranging from 0.9-9.8%, which are rich in iron and magnesium, indicates low-grade metamorphic processes in the geological environment. These minerals are often unstable (Li, *et al*., 2022). As for the group of Garnet minerals, which are considered to be chemically stable minerals that resist weathering. Their percentage ranged from 1.9-7.5%, which indicates that the sediment was far from the source (Scambelluri, 2000). As for the minerals with high resistance to weathering (ultra-stable minerals) such as Zircon, Tourmaline, Rutile they were clearly distinguishable within the study soil, along with other heavy minerals, which showed a noticeable variation in their distribution. These minerals recorded varying ratios ranging from 2.5-8.3% for Zircon and 0-3.3% for Tourmaline. Rutile minerals (0-5.1%), and Staurolite minerals (0-4.8%) most of these minerals are used to determine the age and geological history of parent material, as it is one of the stable minerals that are not easily affected by weathering processes (Gorrfu *et al* 2003; Auer *et al*., 2018). As for Pyroxene minerals, their proportions have been determined to be between 2-7.4%, due to their relative instability, these minerals are susceptible to weathering processes. Amphibole minerals such as hornblende were also characterized by ratios ranging from 2-6.1%, which indicates an undeveloped igneous source. These minerals are subject to fracture at weak zones due to mechanical weathering. Mica minerals, Muscovite (2.3-7.8%) and Biotite (3.4-6.5%), have been identified. The presence of these minerals indicates a short transport distance, and Muscovite is more resistant to weathering compared to Biotite, whose presence indicates a metamorphic volcanic source or a product of rapid decomposition in the sedimentary environment (Bhat and Gupta, 2020). Kyanite is a mineral with high resistance to weathering processes. The results of Table 1 show a decrease in the percentage of study soils, which indicates a weakening of the severity of weathering affecting these soils. The percentage ranged from 0% to 2.6%, and this variation and decrease is due to the influence of the studied soils on geomorphological activities, which in turn influenced the mineral composition of the parent material (Jassin and Goff, 2006). In addition, Epidote (3.9-7.5%), a calcium-rich mineral belonging to Metamorphic volcanic rocks, as well as Celestite (0-1.9%), were diagnosed. Other minerals may include rare or unidentified minerals and may contain components such as Antar, Apatite, and Monazite (Deer *et al*., 2013).

Iraqi Journal of Agricultural Sciences –2026:57(5):1389-1401
P-ISSN: 0075- 0530 /E-ISSN: 2410-0862
DOI: https://doi.org/10.36103/se82k705

Table 1. The percentages of heavy minerals in the sand fraction of the study soil

Heavy Minerals	Sample Numbers																							
	1	2	3	4	5	6	7	8	9	10	11	12	13	14	15	16	17	18	19	20	21	22	23	24	25
Opaques (Iron Oxides)	56.1	49.3	54.9	50.8	52.6	57.0	43.4	46.4	46.6	44.9	42.1	47.6	45.4	41.7	45.7	54.0	46.9	44.9	48.1	44.0	39.1	48.8	48.6	42.7	47.6
Chlorite Group	1.6	1.8	0.9	1.5	3.3	3.1	8.3	7.5	7.0	7.9	9.2	8.0	8.4	8.8	6.8	5.0	6.7	9.8	9.5	8.2	9.2	9.4	9.2	8.9	8.1
Garnet Group	1.9	3.5	2.6	3.0	2.1	2.4	5.7	6.5	5.3	5.2	4.3	5.3	5.7	6.1	5.8	2.7	4.7	5.8	5.4	5.4	4.7	5.3	5.1	7.5	6.2
Zircon	5.8	8.3	7.8	6.4	4.7	3.9	6.7	7.3	5.9	4.8	5.2	3.4	5.3	4.8	4.4	2.5	3.7	5.1	4.5	6.4	6.1	4.4	4.2	4.2	5.8
Pyroxene	3.9	2.5	2.0	2.9	4.1	4.3	6.1	3.1	3.1	6.5	7.4	5.9	6.0	7.4	7.3	4.5	6.2	6.6	3.1	5.9	6.3	5.4	5.2	4.9	4.3
Amphibole	2.0	3.5	3.7	3.3	3.9	4.4	5.9	4.6	3.0	2.5	6.1	4.0	3.2	5.7	3.9	3.9	4.3	4.7	4.8	5.3	6.2	3.0	2.8	5.1	3.1
Epidote	7.5	6.4	5.9	4.4	4.8	3.9	4.7	5.2	5.1	3.9	6.0	6.1	4.6	5.6	4.5	5.3	4.9	4.3	6.2	3.9	5.4	6.1	5.9	5.5	5.3
Biotite	4.3	5.2	3.8	4.7	6.5	4.1	5.9	5.4	3.4	3.9	4.7	4.3	4.6	4.3	4.7	6.5	5.0	4.4	4.5	6.4	6.4	4.4	4.2	5.2	5.1
Muscovite	2.9	2.3	3.4	3.2	4.4	2.7	7.3	4.1	2.4	4.5	4.3	3.4	5.2	3.9	3.4	2.1	3.9	5.1	5.6	7.5	7.8	5.5	5.3	3.5	5.9
Tourmaline	3.1	2.3	3.3	3.0	2.5	3.0	0.8	1.5	2.6	1.5	2.2	1.6	2.2	1.8	1.3	1.0	1.1	2.2	1.9	0.0	0.6	1.8	1.6	1.8	2.9
Staurolite	2.2	4.8	1.7	1.9	1.8	2.4	0.7	2.3	1.9	0.9	1.5	1.9	1.6	1.1	1.6	1.5	1.2	0.4	0.0	0.6	1.2	0.0	0.0	2.1	0.5
Kyanite	1.3	2.0	1.8	1.6	1.9	0.0	0.0	2.4	1.4	1.9	2.6	2.4	2.6	2.2	1.7	1.9	1.7	2.0	1.3	0.0	1.3	1.2	1.0	1.9	2.4
Rutile	2.9	3.9	2.0	2.6	2.3	5.1	0.9	0.0	1.5	1.3	1.0	1.5	1.6	0.6	0.0	0.0	0.0	0.9	0.0	0.4	1.4	0.0	0.0	1.0	0.0
Celestite	1.4	1.4	0.5	1.8	1.5	1.0	0.0	0.6	1.2	1.9	0.0	1.2	0.7	0.0	0.6	1.5	0.5	0.8	1.2	0.0	0.9	1.1	0.9	1.1	1.4
Others	0.9	1.4	1.1	1.6	0.8	1.2	2.2	1.4	1.9	1.2	0.8	1.9	1.7	0.4	1.1	0.9	0.6	1.2	1.4	2.4	2.1	1.3	1.1	1.6	1.3
	97.8	98.6	95.4	92.7	97.2	98.5	98.6	98.3	92.8	92.67	97.4	97.9	98.8	94.3	93.1	93.3	91.4	98.1	97.5	96.8	98.7	97.7	95.6	97.6	99.9

Iraqi Journal of Agricultural Sciences –2026:57(5):1389-1401
P-ISSN: 0075- 0530 /E-ISSN: 2410-0862
DOI: https://doi.org/10.36103/se82k705

2- Maps of the spatial distribution of heavy minerals: The results show that the concentration range of 48.17 to 45.76% to 48.17% covers the largest area in the study region, occupying 32,147.93 hectares, which is 59.04% of the total area. The concentration is 39.11-45.76%, which occupied 17237.04 hectares, 31.66% of the total area of the study region, and the least area represented 9.3% of the total area, which occupied 5066.17 hectares, by concentration 48.17-56.92 % (Figure 2).

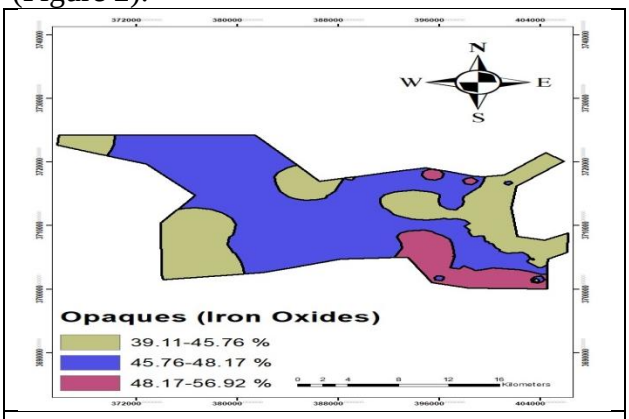

Opaques (Iron Oxides)		
Class Index Value	Area ha	Area %
39.11-45.76	17237.04	31.66
45.76-48.17	32147.93	59.04
48.17-56.92	5066.17	9.3
Area Total	54451.14	

Figure 2. Spatial map of opaque minerals

This can be attributed to the nature of the sediments, their provenance, the intensity of weathering processes they have undergone, and their inheritance from a parent material rich in such minerals (Khedr *et al.,* 2023.). The concentration ranging from (0-4%) showed an area of 486.12 hectares, equivalent to 0.89% of the total area of the study (Figure3), the lowest concentration found in the region. As for the concentration ranging from (7 - 10%), it covers the largest area in the study area, occupying 47,764.49 hectares, equivalent to 87.72% of the total area. While the concentration ranging from 4% to 7% occupies an area of 6200.53 hectares, which is 11.39% of the total area of the district. The variation in the distribution of the proportions of chlorite minerals in the study area reflects the diverse geological formations in the region. The area is located within multiple geological formations, where rocks rich in chlorite, such as metamorphic and sedimentary rocks, are widespread.

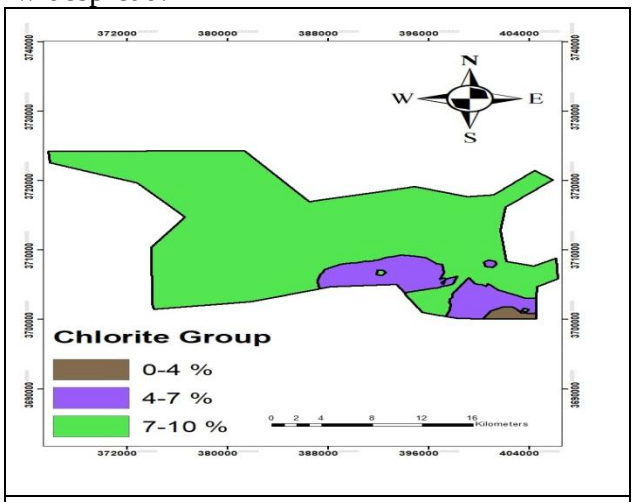

Chlorite Group		
Class Index Value	Area ha	Area %
0-4	486.1157532	0.89
4-7	6200.534309	11.39
7-10	47764.48994	87.72
Area Total	54451.14	

Figure 3. Spatial map of chlorite mineral

This explains the large coverage of the 7-10% concentration in the area. It should be noted that chlorite is a flaky mineral that is formed as a result of metamorphic processes of igneous and sedimentary rocks (Li et al., 2022). The processes of erosion and sedimentation may also play an important role in this variability, and the dry climate of the region limits the decomposition of rocks, allowing the deposition of minerals and their long-term survival. (Blatt *et al.*, 2006; Deer *et al*., 2013). Data from as shown in Figure 4, show that the lowest concentration of Garnet (Garnet Group) (0–3%) covers an area estimated at approximately 306.95 hectares, equivalent to only 0.57% of the total area of the region, and is the least widespread among the identified categories. In contrast, the highest concentration (5–8%) occupies the largest area, covering 47,326.10 hectares, representing 86.91% of the total area, confirming the dominance of this concentration in the region. The intermediate concentration (3–5%) was recorded in an area of 6,818.09 hectares, representing 12.52%.

Iraqi Journal of Agricultural Sciences –2026:57(5):1389-1401
P-ISSN: 0075- 0530 /E-ISSN: 2410-0862
DOI: https://doi.org/10.36103/se82k705

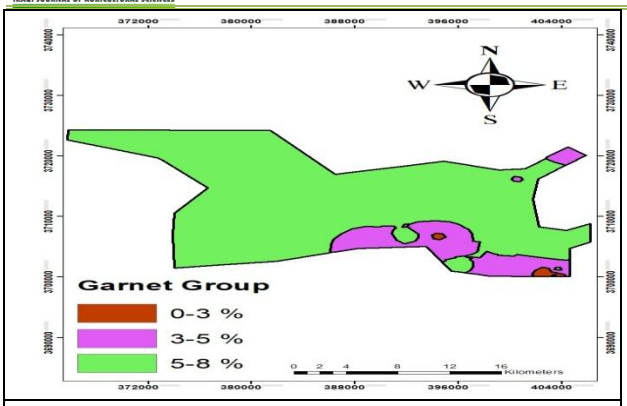

Garnet Group		
Class Index Value	Area ha	Area %
0-3	306.9500046	0.57
3-5	6818.0889	12.52
5-8	47326.1011	86.91
Area Total	54451.14	

Figure 4. Spatial map of Garnet mineral

Garnet is a silicate mineral that often occurs in high-temperature and pressure environments, particularly during metamorphic processes affecting metamorphic and volcanic rocks (Nesse, 2012). Given the diversity of rock formations in the region, ranging from sedimentary to metamorphic, the variation in Garnet concentrations is attributed to the interaction of several geological and environmental factors, including the nature of the rocks, ancient tectonic activity, erosion and sedimentation processes, and the influence of the region's dry climate. The analysis results shown revealed a significant variation in the percentages of Zircon in the soil samples taken from the study area. The accompanying Figure 5 shows that most of the area falls within the 3% to 6% Zircon concentration category. This category covers approximately 52,459.52 hectares, or approximately 96.34% of the total area. The lowest prevalence was recorded within the 0% to 3% category, covering an area of no more than 152.97 hectares (0.28%). The highest category (6–9%) covered an area of 1,838.64 hectares, equivalent to 3.38%. Zircon is known as a silicate mineral rich in zirconium and is characterized by its high resistance to decomposition and alteration, both physical and chemical (Nugraha *et al*., 2024). The abundance of Zircon in the region is attributed to environments that experienced long periods of sedimentary stability, such as ancient river courses that were not subject to active erosion (Auer *et al.*, 2018; Chen *et al*., 2024). Given the nature of the Karma region, which contains sedimentary formations dating back to ancient times, it is likely that the sedimentation processes accumulated in these environments contributed to the preservation and concentration of this mineral in the current soil (Zhang *et al.*, 2020; Nugraha *et al*., 2024).

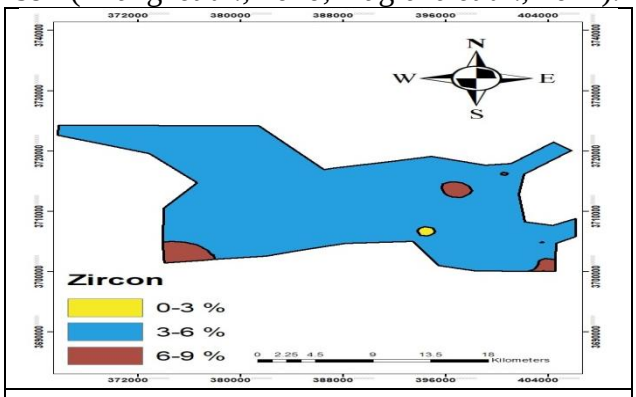

Zircon		
Class Index Value	Area ha	Area %
0-3	152.9732666	0.28
3-6	52459.52469	96.34
6-9	1838.642044	3.38
Area Total	54451.14	

Figure 5. Spatial map of Zircon mineral

Figure 6 shows that the percentages of Pyroxene, according to the spatial distribution shown on the Figure,6 cover the largest area, covering approximately 34,346.18 hectares, representing approximately 63.08% of the region's area. Meanwhile, the concentration between 3% and 5% covers an area of 20,015.59 hectares, representing 36.76%. The lowest recorded percentage is for the 0% to 3% category, covering an area of no more than 89.38 hectares, representing 0.16%. The presence of Pyroxene in soil is linked to several natural factors, as it is a common mineral in igneous rocks such as basalt and gabbro. It is likely that the region was previously affected by tectonic activity that contributed to the introduction of these rocks into the current sedimentary environment. The region's passage through various stages of intense erosion over time, along with its being part of a relatively low-lying environment or flood zones, has helped in the accumulation of pyroxene and the variation in its proportions from one location to another (Al-Bassam *et al*., 2006).

Iraqi Journal of Agricultural Sciences –2026:57(5):1389-1401
P-ISSN: 0075- 0530 /E-ISSN: 2410-0862
DOI: https://doi.org/10.36103/se82k705

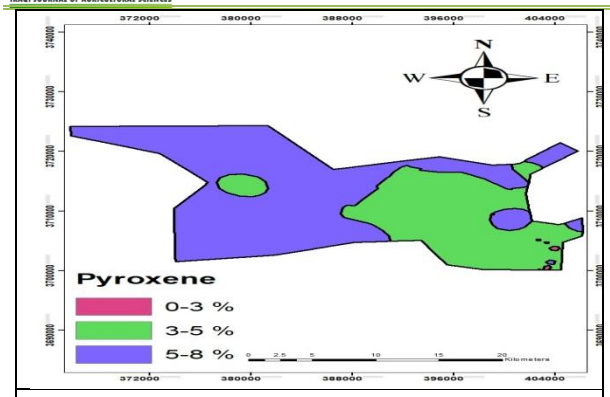

Pyroxene		
Class Index Value	Area ha	Area %
0-3	89.37810469	0.16
3-5	20015.58667	36.76
5-8	34346.17523	63.08
Area Total	54451.14	

Figure 6. Spatial map of Pyroxene mineral

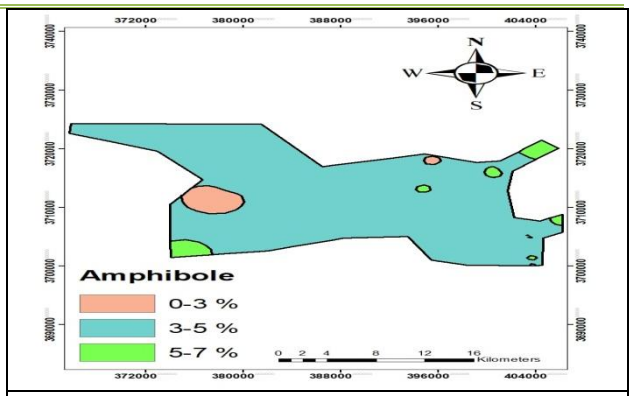

Amphibole		
Class Index Value	Area ha	Area %
0-3	1957.144	3.59
3_5	50682.74	93.08
5_7	1811.258	3.33
Area Total	54451.14	

Figure7. Spatial map of Amphibole mineral.

The results shown that Amphibole, according to the geographical distribution displayed in Figure7, accounts for the largest proportion of the area in the 3% to 5% concentration category, covering approximately 50,682.74 hectares, equivalent to 93.08% of the total area. This is followed by the low concentration category (0–3%), which occupies approximately 1,957.14 hectares (3.59%), while the smallest area is recorded in the high concentration category (5–7%), which covers only 1,811.26 hectares, equivalent to 3.33% of the total area. Although the dominant formations in the Karma area consist of sedimentary rocks and carbonate components dating back to the Cretaceous and Eocene periods, the occurrence of amphibole levels, especially in areas with higher concentrations, may indicate the presence of pockets of igneous or metamorphic rocks in the deeper layers of the soil, or sedimentary transport processes caused by erosion from neighboring areas rich in these rocks. The Euphrates River, which runs near the study area, may have contributed to the deposition of sediments containing this mineral, reinforcing the hypothesis that the current distribution is linked to ancient geological events and the diversity of sedimentary sources (Jassin and Goff. 2006; Velde, 2020).

An analysis of the distribution of Epidote in the soil of the study area, the data shows that the medium concentration category (4-6%) predominates, covering an area of approximately 53,164.00 hectares, which constitutes 97.64% of the total area of the studied region. In contrast, the low concentration category (0–4%) covers an area estimated at 6,740.73 hectares, representing 1.36%. The highest concentration category (6-8%) is the least widespread, covering an area of only 546.40 hectares, equivalent to only 1% of the total area .Figure (8) accurately illustrates this spatial distribution, reflecting the pattern of accumulation of this mineral within the geological and environmental conditions prevailing in the region.

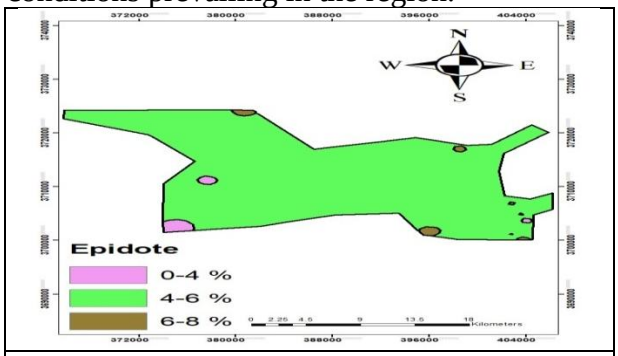

Epidote		
Class Index Value	Area ha	Area %
0-4	740.7321386	1.36
4_6	53164.0029	97.64
6_8	546.4049649	1
Area Total	54451.14	

Figure 8. Spatial map of Epidote mineral

Iraqi Journal of Agricultural Sciences –2026:57(5):1389-1401
P-ISSN: 0075- 0530 /E-ISSN: 2410-0862
DOI: https://doi.org/10.36103/se82k705

The widespread distribution of Epidote within the medium concentration category reflects interconnected environmental and geological influences. This mineral typically occurs in metamorphic rocks, particularly green schist, which develop under moderate temperature and pressure conditions an ideal environment for Epidote formation. Its presence also suggests the presence of ancient rock units of igneous or metamorphic origin at depth. This distribution can also be attributed to sediment transport by the Euphrates River, which contributed to the redisposition of mineral materials in the surrounding plains. Furthermore, the removal of surface layers by erosion may have helped expose or accumulate quantities of this mineral in specific areas of the soil (Dehghani *et al*., 2022). In Figure 9, it appears that Muscovite occupied the largest proportion of the area in the medium concentration category (3–6%), covering approximately 50,309.83 hectares, and representing 92.39% of the total area. Concentrations between 0–3% covered a smaller area of 1,537.23 hectares (2.83%), while the highest concentration (6–9%) extended over 2,604.08 hectares, equivalent to 4.78% of the total area (Figure9). The distribution of muscovite in the region reflects a direct influence of its rock composition, as the presence of feldspar-rich rocks such as Garnet, in addition to metamorphic rocks such as schist, contributes to the high concentration of this mineral (AlKhalil, 2025.). Muscovite is typically formed through the chemical weathering of rocks containing aluminum-rich silicate minerals. However, the dry climate in the study area limits the effectiveness of these processes, allowing muscovite to remain in the soil for longer periods of time without decomposition. Environmental changes caused by human activities such as agriculture and construction may also contribute to reducing the concentration of this mineral in some locations by removing or mixing surface layers.

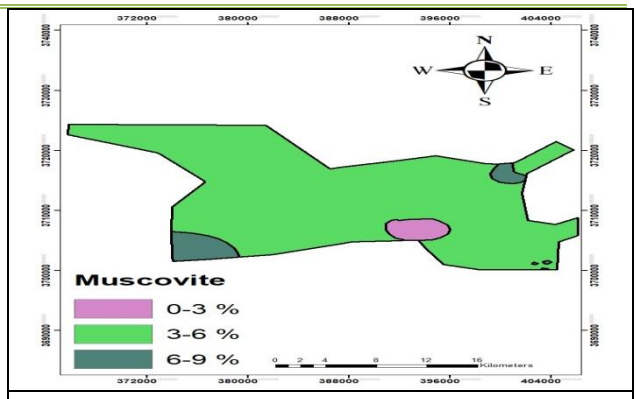

Muscovite

Class Index Value	Area ha	Area %
0-3	1537.227781	2.83
3_6	50309.83615	92.39
6_9	2604.076067	4.78
Area Total	54451.14	

Figure 9. Spatial map of Muscovite mineral

The study showed that the distribution of Biotite in the soils of the Karma region is mostly concentrated in the medium concentration category (4-6%), covering approximately 96.82% of the area, or 52,720.32 hectares. Higher concentrations (6-8%) do not exceed 2.33% of the area, while lower concentrations (0-4%) constitute a small percentage, estimated at 0.85% (Figure10)**.** This limited distribution of biotite indicates that the region's rocks, particularly igneous ones, are relatively devoid of mica minerals. This is attributed to the relatively quiet geological nature of the Karma region, which has not experienced extensive thermal or volcanic activity in recent geological periods. However, the presence of small proportions of this mineral may reflect the effects of ancient thermal transformations or previous geological activities, while the dry climate limits chemical decomposition processes, which contributes to the stability of Biotite within the surface layers (Brewer, 1976).

Iraqi Journal of Agricultural Sciences –2026:57(5):1389-1401
P-ISSN: 0075- 0530 /E-ISSN: 2410-0862
DOI: https://doi.org/10.36103/se82k705

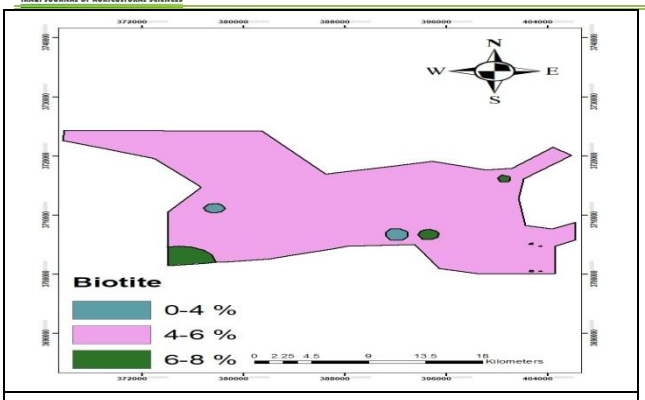

Biotite		
Class Index Value	Area ha	Area %
0-4	459.8984	0.85
4_6	52720.32	96.82
6_8	1270.924	2.33
Area Total	54451.14	

Figure10. Spatial map of Biotite mineral

The distribution of Tourmaline in the soil of the study area showed that the low concentration category (0-3%) predominated, covering an area estimated at 32,667.49 hectares, representing approximately 59.99% of the total area. The medium concentration category (3–6%) occupies an area of 18,114.85 hectares, representing 33.27% of the total area**.** The highest concentration category (6-9%), meanwhile, has the smallest area, covering only 3,668.81 hectares, representing only 6.74% of the total area (Figure11). Tourmaline is a complex, multicolored silicate mineral that often forms. Its presence in surface sediments is associated with erosion processes that transport remnants of parent rocks, as well as deposition in closed or geologically stable environments. This uneven distribution clearly reflects the diversity of rock sources in the region, along with environmental and geomorphological factors that have contributed to the concentration of this mineral in some locations and not others (Gorrfu *et al.*, 2003; Auer *et al.*, 2018; Chakraborty, 2021).

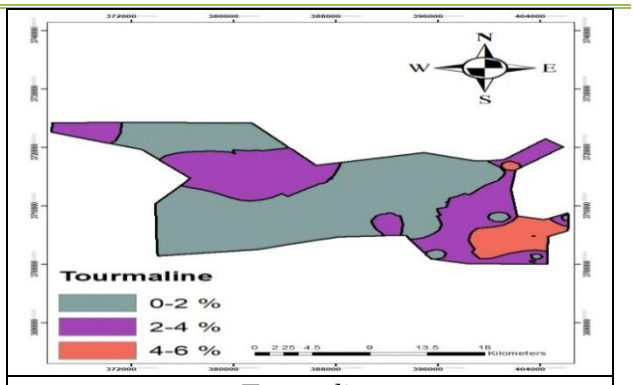

Tourmaline		
Class Index Value	Area ha	Area %
0-3	32667.48535	59.99
3_6	18114.84872	33.27
6_9	3668.805926	6.74
Area Total	54451.14	

Figure 11. Spatial map of Tourmaline mineral

The attached map (Figure 12) shows a clear variation in Staurolite concentrations within the study area. The highest concentration was between (4- 6%), covering an area estimated at 1,425.86 hectares, representing only 2.62% of the total area. In contrast, the category with a concentration ranging (2-4%) represents the largest proportion of the area, covering an area of 32,508.41 hectares (59.7%). The category with the lowest concentration (0-2%) covers an area of 20,516.87 hectares, equivalent to 37.68%. This distribution is closely related to the geological structure, .In addition, river transport, particularly from the nearby Euphrates River, contributes to the redistribution of minerals through river sediments, which supply the study areas with materials rich in this type of mineral (Nesse, 2012).

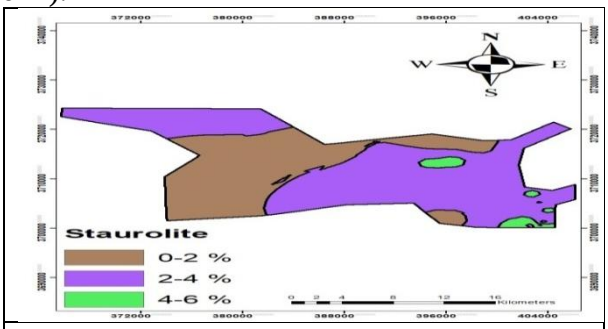

Staurolite		
Class Index Value	Area ha	Area %
0-2	20516.86621	37.68
2_4	32508.41539	59.7
4_6	1425.858394	2.62
Area Total	54451.14	

Figure12. Spatial map of Staurolite mineral

Iraqi Journal of Agricultural Sciences –2026:57(5):1389-1401
P-ISSN: 0075- 0530 /E-ISSN: 2410-0862
DOI: https://doi.org/10.36103/se82k705

The distribution of Kyanite in the study area appears within three main concentration categories, range (0-3%)The low concentration category (0–1%) covers approximately 3,086.65 hectares, representing 5.67% of the total area, while the medium concentration category (1–2%) is the most widespread, covering an area of 30,683.83 hectares, representing 56.35%. The highest concentration category (2-3%) occupies approximately 20,680.66 hectares, representing 37.98% (Figure 13). This geographical variation in Kyanite concentration is linked to structural factors and the geological history of the region, as the mineral is an indicator of aluminum-rich metamorphic rocks formed under high pressures and temperatures. Tectonic activity in some parts of the region may have contributed to the crystallization and redistribution of minerals, while erosion and river transport influence its transport and deposition in the adjacent plain environments (Cottle *et al*., 2022).

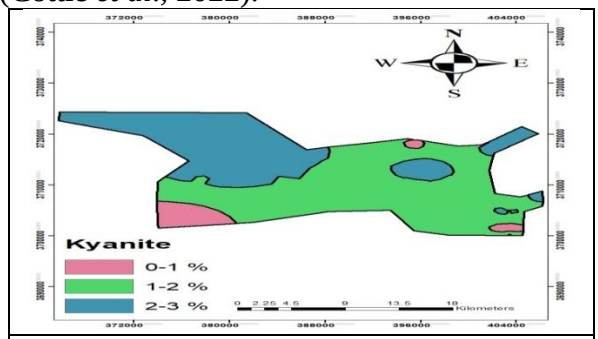

Kyanite		
Class Index Value	Area ha	Area %
0-1	3086.646667	5.67
1_2	30683.82976	56.35
2_3	20680.66357	37.98
Area Total	54451.14	

Figure 13. Spatial map of Kyanite mineral

The results show that the distribution of Rutile in the study area is marked by a significant presence within the 4-6% concentration category. This category covers an area estimated at approximately 4,743.55 hectares, representing 8.71% of the total area. This concentration is considered the lowest in the region. The concentration ranging from 0-2% covers the largest area of the study area, occupying approximately 31,933.21 hectares, equivalent to 58.65% of the total area. The concentration ranging from 2-4% covers 17,774.38 hectares, equivalent to 32.64% of the total area (Figure14). The presence of rutile in the Karma area reflects a geological environment rich in heavy minerals because of river transport and flood sedimentation. The variation in rutile concentrations in the region also indicates that mechanical sorting played a significant role in the distribution of heavy sediments. The Euphrates River, which flows close to the area, is a contributing factor in the transport and deposition of mineral sediments, depending on the strength of the water currents. This has led to the accumulation of rutile in some areas at higher rates than others. Most of the area has low concentration, indicating that the region is not very rich in this mineral. However, its general prevalence is evident because of transport processes, reflecting the significant influence of river transport and alluvial sediments on the region (Nesse, 2012).

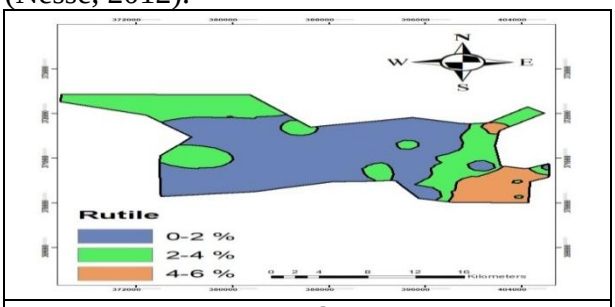

Rutile		
Class Index Value	Area ha	Area %
0-2	31933.20908	58.65
2_4	17774.37617	32.64
4_6	4743.554749	8.71
Area Total	54451.14	

Figure 14. Spatial map of Rutile mineral

The results shown that the Celestite concentration ranging from 0-1% covers an area of 3,652.6 hectares, equivalent to 6.71% of the total area of the study area, which is considered the lowest concentration in the region. The concentration ranging from 1-2% covers the largest area, extending over 31,359.96 hectares, equivalent to 57.59% of the total area. Meanwhile, the concentration ranging from 2-3% covers an area of 19,438.58 hectares, equivalent to 35.7% of the total area of the study area, as shown in Figure15. Celestite is characterized by its presence in sedimentary environments rich in sulfates, as it is usually found in layers of sulfate rocks and geological formations rich in

Iraqi Journal of Agricultural Sciences –2026:57(5):1389-1401
P-ISSN: 0075- 0530 /E-ISSN: 2410-0862
DOI: https://doi.org/10.36103/se82k705

this mineral. These accumulations result from long-term sedimentation processes, and their presence may be due to the presence of groundwater rich in sulfates, which enhances the accumulation of this mineral in these sedimentary environments (Mange and Maurer, 1992).

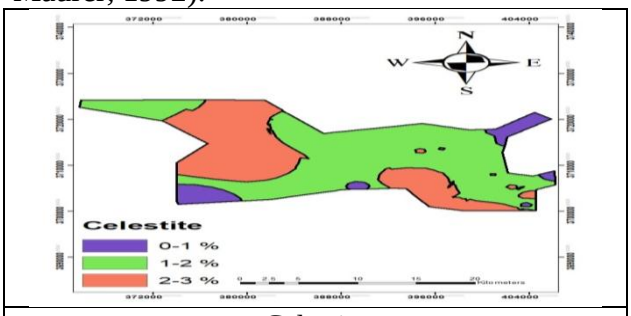

Celestite		
Class Index Value	Area ha	Area %
0-1	3652.60365	6.71
1_2	31359.95509	57.59
2_3	19438.58126	35.7
Area Total	54451.14	

Figure15. Spatial map of Celestite mineral

CONCLUSION

The study examined the mineral composition of surface soils in the Al-Karmah area within the Euphrates floodplain in western Iraq. Heavy and light minerals were separated and identified using polarized microscopy, while GIS techniques were applied to analyze their spatial distribution. The results showed the dominance and widespread distribution of iron oxides, chlorite, garnet, zircon, pyroxene, amphibole, epidote, muscovite, and biotite. These mineral patterns reflect the effects of parent materials, sedimentary deposition, and weathering processes in the study area.

JOURNAL DECLARATION

The First author (**Shireen Mudhafar Ali Alkhalil**) serves as an editor for Iraqi Journal of Agricultural Sciences but was not involved in the peer review process of this manuscript beyond their role as an author. The authors declare no other conflict of interest.

ACKNOWLEDGEMENT

The authors would like to express their sincere appreciation to all individuals and institutions that supported this study and contributed to the completion of the research work.

CONFLICT OF INTEREST

The authors declare that they have no conflicts of interest.

AUTHOR/S DECLARATION

We confirm that all Figures and Tables in the manuscript are original. Any Figures or images adopted from other sources were used with the necessary permissions for re-publication.

All authors have approved the final version of the manuscript.

Ethical Clearance and Animal Welfare: Not applicable.

Funds: This research received no external funding.

AUTHOR'S CONTRIBUTION STATEMENT

All authors contributed to the study conception, data collection, laboratory analysis, interpretation of results, manuscript writing, and final approval of the submitted version.

REFERENCES

Bassam, K.S., A.I. Al-Juboury, and T. Al-Ani. 2006. Heavy minerals in the recent sediments of the Euphrates River, Western Iraq. Iraqi Bulletin of Geology and Mining, 2(2):33–42. https://ibgm-iq.org/ibgm/index.php/ibgm/article/view/74.

AlKhalil, SH. M. A 2025. Weathering indices and mineralogical composition of the sand fraction in soils from the western desert of holy Karbala governorate, Iraq. Applied Chemical Engineering 8 (4): https://doi.org/10.59429/ace.v8i4.5760

Auer, M., R. Deguise, and S. White. 2018. Zircon and tourmaline as geochronological tools: applications in metamorphic and igneous rocks. Journal of Geology, 126(3), 305-320. https://doi.org/10.1086/693246.

Brewer, R. 1976. Fabric and Mineral Analysis Of Soils. Robert E.Krieger publishing company. Huntington.N.Y

Bhat, S. M., and P.K. Gupta. 2020. Geochemistry and petrology of mica-bearing rocks. Journal of Earth Sciences, 34(4): 512-525. https://doi.org/10.1016/j.jes.2020.02.004.

Blatt, H., G. Middleton, and R. Murray. 2006. Origin Of Sedimentary Rocks 4thed. Prentice Hall. pp:643.

Chakraborty, T. 2021. Tourmaline growth and evolution in S-type Garnets and pegmatites: constraints from textural, chemical and B-isotopic study from the Gangpur Schist Belt granitoids, eastern India. Geological Magazine, 158(9):1657–1670. https://doi.org/10.1017/S0016756821000224

Iraqi Journal of Agricultural Sciences –2026:57(5):1389-1401
P-ISSN: 0075- 0530 /E-ISSN: 2410-0862
DOI: https://doi.org/10.36103/se82k705

Chen, H., C. Zhang, X. Liu, Y. Dong, X.Tan, Q.Chen, Z. Zhang, and K.Wei, .2024. Detrital zircon u-pb geochronology and provenance of silurian, devonian and permian sedimentary rocks, south qinling: constraints on late palaeozoic tectonic evolution history of the qinling orogenic belt. Geological Journal, 59(3):811–837. https://doi.org/10.1002/gj.4893.Wiley Online Library

Cottle, J.M., K.P. Larson and D.A. Kellett. 2022. Kyanite petrogenesis in migmatites: resolving melting and metamorphic signatures. Contributions to Mineralogy and Petrology, 177(2): 1–20. https://doi.org/10.1007/s00410-022-01991-w

Deer, W.A., R.A. Howie and J. Zussman .2013. An Introduction to the Rock-Forming Minerals (3rd ed.). Mineralogical Society.

Dehghani, A., M. Yousefi and E. Asadi, .2022. Petrological and geochemical characteristics of epidote-bearing rocks: Implications for metamorphic processes. Lithos, 288, 105803. https://doi.org/10.1016/j.lithos.2022.105803 .

Gorrfu, B. H., M.D. Roeser and M. Lee, .2003. Zircon and Tourmaline as indicators of metamorphic history in the Mozambique Belt. Geological Journal, 38(1): 1-14. https://doi.org/10.1002/gj.978

Hesse, P.R. 1971. A text Book of Soil Chemical Analysis. 1st ed. John Murray. LTD. London, British .pp:556 . https://indianecologicalsociety.com/wp-content/themes/ecology/volume_pdfs/page-20.pdf

Issa, S. K. 2022. Minerals of the soil. Ministry of Higher Education and Scientific Research, Iraq.pp:249.

Jassin, R., and W. Goff. 2006. Mineralogy of amphibole-bearing rocks: Implications for tectonic settings. Journal of Mineral Science, 52(1): 97-108. https://doi.org/10.1016/j.minsci.2006.02.004.

Jubair, A.R., N.F.Abboud, and A. G.I Hamad. 2019. Horizontal variability of some soil properties in wasit Governorate by using time series analysis. Indian Journal of Ecology :46(3):558-566. https://indianecologicalsociety.com/wp content/themes/ecology/volume_pdfs/page-20.pdf

Khedr, M. Z., H. Zaghloul, E. Takazawa, H. El-Nahas, M. K. Azer and S.A. El Shafei. 2023. Genesis and evaluation of heavy minerals in black sands: A case study from the southern Eastern Desert of Egypt. Chemie der Erde – Geochemistry, 83(1): 125945. https://doi.org/10.1016/j.chemer.2022.125945

Li, C., P. Shen, Y. Zhao, P. Li, L. Zhang, and H. Pan. 2022. Mineral chemistry of chlorite in different geologic environments and its implications for porphyry Cu ± Au ± Mo deposits. Ore Geology Reviews, 145, 105112. https://doi.org/10.1016/j.oregeorev.2022.105112

Mange, M. and H. Maurer. 1992. Heavy minerals of the earth's crust and their use in sedimentary environments. Geological Review, 75(2): 181-190. https://doi.org/10.1007/BF02875299

Nesse, W. D. 2012. Introduction to Mineralogy 2nded. Oxford University Press.pp:496.

Nugraha, A. M. S., J. Hennig-Breitfeld, R. Puspita, A. D. Switzer and R. Hall. 2024. Detrital zircons and heavy minerals from the palu formation, Sulawesi, Indonesia: constraints on exhumation of the palu metamorphic complex and drainage evolution. Journal of the Geological Society, 181(3):2023-118. https://doi.org/10.1144/jgs2023-118.Geoscience World

Saber, M., W. M. Saod, and E.A. Al-Heety. 2021. Vertical and lateral distribution of heavy minerals in the Euphrates river sediments between Heet and Fallujah, Western Iraq. Iraqi Geological Journal, 54(2A):112–123. https://doi.org/10.46717/igj.54.2A.9Ms-2021-07-30.

Scambelluri, M. 2000. Pressure, temperature, fluid pressure conditions of metamorphism. (n.d.). In Encyclopedia of Life Support Systems (EOLSS). EOLSS Publishers.pp:15 https://www.eolss.net/Sample-Chapters/C01/E6-15-03-08.pdf

Velde, B. 2020. Amphiboles in geological processes. Earth Science Reviews, 196,102874. https://doi.org/10.1016/j.earscirev.2019.102874

Zhang, J., H. Chen, Y. Yang, G.Tang, C. Li, and F. Wu, .2020. Large Zr isotope variations in single zircon grains record magmatic evolution. Proceedings of the National Academy of Sciences, 117(39): 24010–24016.

Iraqi Journal of Agricultural Sciences –2026:57(5):1389-1401
P-ISSN: 0075- 0530 /E-ISSN: 2410-0862
DOI: https://doi.org/10.36103/se82k705

التغاير المكاني لمعادن الرمل الثقيلة في منطقة الكرمة – محافظة الانبار، العراق

شيرين مظفر علي الخليل، بلال مجيد كريم المشهداني، عبد الغفور ابراهيم حمد، سوسن محمد احمد

المستخلص

هدف هذه الدراسة إلى تحليل التركيب المعدني في منطقة الكرمة بمحافظة الأنبار غرب العراق، ضمن السهل الفيضي لنهر الفرات، والمحصورة بين دائرتي عرض "33°23'00 و "33°25'00 شمالاً، وخطي طول "43°53'00 و "43°56'00 شرقاً، بمساحة تبلغ 54451.14 هكتار. تم جمع 25 عينة من التربة السطحية بعمق يتراوح بين 0 و30 سم، استخدمت البروموفورم لفصل المعادن الثقيلة عن الخفيفة، وشُخِّص تركيبها المعدني باستخدام المجهر المستقطب. ثم أُدخلت البيانات إلى برنامج GIS ArcMap لتحليل التوزيع المكاني وإنتاج خرائط باستخدام طريقة IDW ظهرت نتائج التحليل الجغرافي لتوزيع المعادن الثقيلة في تربة منطقة الكرمة سيادة نسب محددة لعدد من المعادن. فقد غطت أكاسيد الحديد بنسبة (45.76–48.17%) أكبر مساحة بلغت 59.04%. بينما سجل الكلورايت نسبة (7–10%) في 87.72% من المنطقة. سيطر الكرانيت بنسبة (5–8%) على 86.91%، والزركون (3–6%) على 96.34%. البيروكسين (5–8%) غطى 63.08%، والأمفيبول (3–5%) سجل 93.08%. أما الإبيدوت (4–6%) فقد بلغ 97.64%. وجد المسكوفايت بنسبة (3–6%) في 92.39%، في حين بلغت نسبة البيوتايت (4–6%) على 96.82% من المساحة.

الكلمات المفتاحية: طريقة معكوس المسافة IDW .المعدني، المجهر المستقطب.